Electronic Supplementary Material (ESI) for Soft Matter.

Supporting Information

Ag-induced Metallogel Based on Cyclooctatetrathiophene: Structural Characterization and Stimuli-responsive Properties

Yu Tian, [§a] *Chenglong Wang,* [§a] *Guangxia Wang*[a] Li Xu[b] and Hua Wang*[a]*

[a] Engineering Research Center for Nanomaterials, Henan University, Kaifeng, 475004, China.
[b] College of Chemistry and Chemical Engineering, Henan University, Kaifeng 475004, China.

E-mail address: wangguangxia@henu.edu.cn and hwang@henu.edu.cn

Table of Contents

1. General Procedures and Materials

All starting chemicals were obtained from commercial sources and used without further purification. Anhydrous tetrahydrofuran (THF) was distilled sodium benzophenone under argon. Concentration of *n*-BuLi (in hexane) was determined by titration with N-pivaloyl-*o*-toluidine.[S1] Compounds **4**[S2] and **5**[S3] were prepared as previously reported. Column chromatography was carried out on silica gel using 200-300 mesh. Analytical thin-layer chromatography (TLC) was performed using precoated TLC plates with silica gel GF-254.

NMR spectra were obtained with a Bruker spectrometer (^{1}H, ^{13}C, Bruker AVANCE 400 MHz) using chloroform-*d* ($CDCl_3$), acetone-d_6 or the mixture of them as solvent. The chemical shift references were as follows: (^{1}H) chloroform-*d*, 7.26 ppm; (1H) acetone-d_6, 2.05 ppm; (^{13}C) chloroform-*d*, 77.16 ppm. IR spectra were recorded on FT-IR spectrometer with thin KBr disk. High resolution mass spectra ESI were acquired on FT-ICR spectrometer. Melting point determination was taken on a Melt-Temp apparatus and was uncorrected. UV-vis spectra were obtained with a double-beam spectrophotometer at room temperature. PL were obtained with Shanghai Prism F97. TEM images were obtained on a JEM-2010 trasmission electron microscope oppereting at an accelerating voltage of 200 kV by drop casting the sample dispersion on copper grids coated with a carbon film. SEM images were obtained on a Carl Zeiss GEMINI500 electron microscope operating at an accelerating voltage of 5.0 kV after the sample was coated with a thin layer of gold. XPS data of samples were collected on Thermo Scientific Escalab 250Xi X-ray photoelectron spectroscopy. Rheological measurements were performed on a Rotational Rheometer (DHR2) with parallel plate geometry. AFM images were collected on Scanning probe microscope (Dimension Icon) in tapping mode by the probe of 3 N • m^{-1} using 0.99 Hz scan rate at environment.

2. Syntheses of New Compounds

Scheme S1. Synthesis of Ligands 2 and 3 [a].

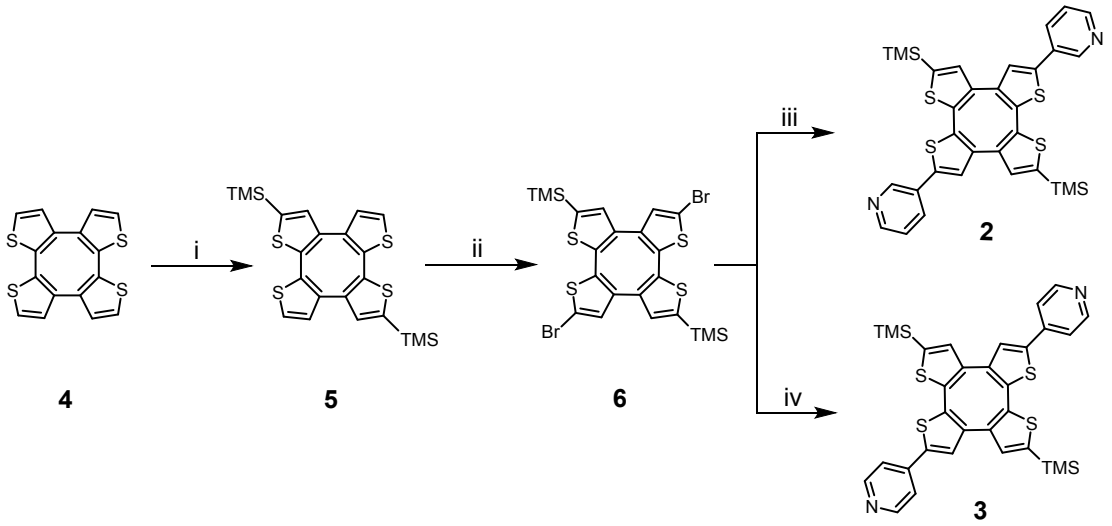

[a]Reagents and conditions: (ⅰ) *n*-BuLi, THF, -78 ℃ for 2 h, then TMSCl, -78 ℃ to rt for 12 h; (ⅱ) *n*-BuLi, THF, -78 ℃ for 2 h, then $C_2Br_2Cl_4$, -78 ℃ to rt for 12 h; (ⅲ) pyridine-3-boronic acid, $Pd(PPh_3)_4$, K_2CO_3, THF, 80 ℃ for 12 h; (ⅳ) pyridine-4-boronic acid, $Pd(PPh_3)_4$, K_2CO_3, THF, 80 ℃ for 12 h.

Synthesis of compound 6.

n-BuLi (2.47 M, 0.46 mL, 1.15 mmol) was added dropwise to a solution of **5** (258 mg, 0.55 mmol) in dry THF (35 mL) at -78 ºC under an argon atmosphere. After the mixture was stirred at -78 ºC for 2 h, 1,2-dibromo-1,1,2,2-tetrachloroethane (444 mg, 1.36 mmol) was added to the mixture at the same temperature, and then the solution was warmed to room temperature overnight. After the reaction was quenched with methanol at -78 ºC, the reaction mixture was concentrated under reduce pressure. The crude product was extracted with dichloromethane and water and dried over anhydrous $MgSO_4$. After removing the solvent, the residue was purified by silica gel column chromatography (petroleum ether), and then the resultant solid was washed with methanol to give compound **6** as a white solid (326 mg, 95%). M.p. 220-221 ºC. IR (KBr): 2954, 1450, 1250, 986, 841 cm^{-1}. ^1H NMR (400 MHz, $CDCl_3$, 298 K): δ 6.99 (s, 1H), 6.96 (s, 1H), 0.31 (s, 9H). ^{13}C NMR (100 MHz, $CDCl_3$, 298 K): δ 143.86, 137.21, 136.91, 136.52, 136.48, 133.53, 132.59, 113.97, -0.09. HRMS (ESI) m/z calcd

for $C_{22}H_{23}Br_2S_4Si_2^+$ $(M+H)^+$ 628.85824, found 628.85785.

Synthesis of compounds 2 and 3.

A mixture of **6** (160 mg, 0.25 mmol), pyridine-3-boronic acid (69 mg, 0.56 mmol) $Pd(PPh_3)_4$ (15 mg, 0.01 mmol), and K_2CO_3 (175 mg, 1.27 mmol) in THF (20 mL) and H_2O (4 mL) was stirred under Ar atmosphere for 12 h at 80 ℃. The solution was concentrated under reduce pressure. The crude product was extracted with dichloromethane and water, dried over anhydrous $MgSO_4$. After removing the solvent, the residue was purified by silica gel column chromatography (dichloromethane / methanol = 300:1) to afford **2** as a yellow solid (103 mg, 65%). M.p. 210-211 ºC. IR (KBr): 2926, 1633, 1411, 1251, 980, 840, 704 cm^{-1}. ^1H NMR (400 MHz, $CDCl_3$) δ 8.87 (d, J = 1.5 Hz, 1H), 8.53 (d, J = 4.3 Hz, 1H), 7.85 (m, 1H), 7.32 (m, 1H), 7.12 (s, 1H), 0.35 (s, 9H). ^{13}C NMR (100 MHz, $CDCl_3$) δ 148.96, 146.79, 143.62, 141.59, 137.89, 137.50, 137.22, 136.71, 132.90, 132.76, 129.95, 127.07, 123.83, -0.06. HRMS (ESI) m/z calcd for $C_{32}H_{31}N_2S_4Si_2^+$ $(M+H)^+$ 627.09031, found 627.09058.

Compound **3** was synthesized in a similar way to that described for **2**. The residue was purified by silica gel column chromatography (dichloromethane / methanol = 150:1) to afford **3** as a yellow solid in the yield of 71%. M.p. 196-197 ºC. IR (KBr): 2955, 1596, 1410, 1251, 984, 841 cm^{-1}. ^1H NMR (400 MHz, $CDCl_3$) δ 8.60 (d, J = 5.9 Hz, 2H), 7.45 (dd, J = 4.7, 1.4 Hz, 2H), 7.40 (s, 1H), 7.11 (s, 1H), 0.36 (s, 9H). ^{13}C NMR (100 MHz, $CDCl_3$) δ 150.59, 144.06, 142.16, 140.86, 137.86, 137.35, 137.25, 136.71, 134.10, 128.09, 119.52, -0.07. HRMS (ESI) m/z calcd for $C_{32}H_{31}N_2S_4Si_2^+$ $(M+H)^+$ 627.09031, found 627.09076.

3. Crystal Structure of Compound 1 and Crystal Data of Compounds 2 and 3

X-ray Single crystal diffraction for Compounds **1-3** data were performed on a diffractometer with CCD detector using Mo Kα radiation (λ= 0.71069 Å) or Cu Kα radiation (λ= 1.54178 Å) source. Their structures were solved by direct methods using SHELXTL and refined with full-matrix least-squares calculations on F^2 using SHELXL-97. All non-hydrogen atoms were refined anisotropically. All hydrogen atoms were positioned by geometric idealization. Additional crystal data and refinement information were summarized in Table S1.

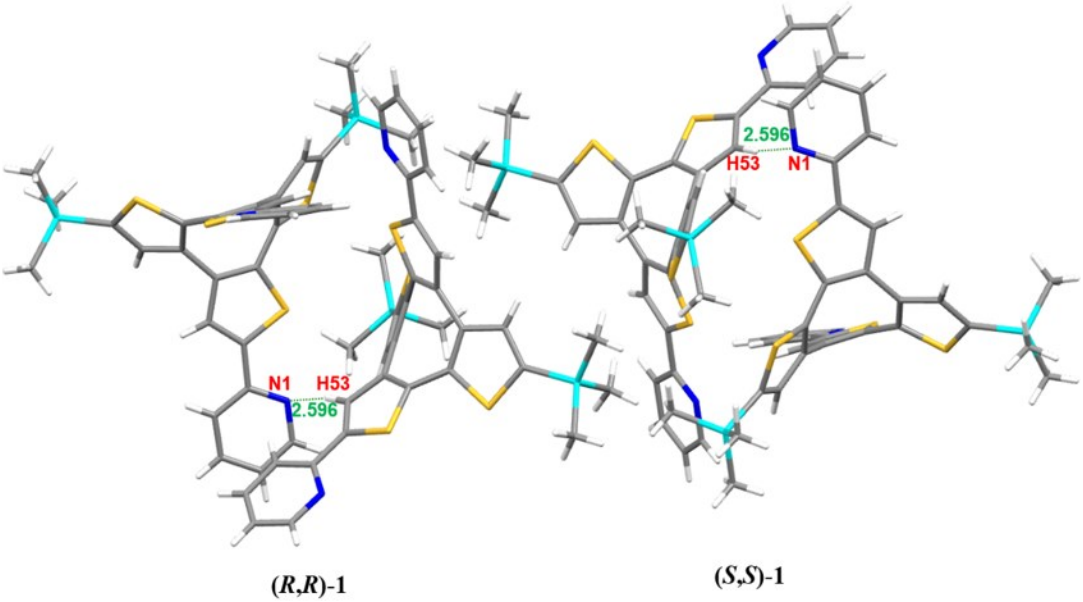

Figure S1. The packing pattern of crystal structure of ligand **1** which crystallized from chloroform and acetonitrile.

Table S1. Crystal data and structure refinement for **2** and **3**.

compound	**2**	**3**
Formula	$C_{32}H_{30}N_2S_4Si_2$	$C_{32}H_{30}N_2S_4Si_2$
fw	627.00	627.00
Temp (K)	293(2)	300.51
crystal system	Triclinic	Triclinic
space group	P-1	R-3
a (Å)	10.1836(8)	38.5368(12)
b (Å)	16.2598(12)	38.5368(12)
c (Å)	23.1451(14)	13.3783(8)
α (deg)	86.414(5)	90
β (deg)	81.109(6)	90
γ (deg)	77.472(6)	120
V (Å^3)	3694.6(5)	17206.1(15)
Z	4	21
D_c (g/cm^3)	1.127	1.089
μ (mm^{-1})	0.344	0.332
F (000)	1312.0	5904.0
reflns collected	89991	88922
unique reflns (R_{int})	0.1207(0.0760)	0.0810(0.0305)
θ range (deg)	7.246-52.042	5.754-49.996
data/restraints/params	14336/30/733	6714/0/367
final R indices	0.0805/0.1835	0.0369/0.0843
R indices (all data)	0.1241/0.2044	0.0641/ 0.1021
GOF on F^2	1.015	1.092
ρ_{max}/ρ_{min}(e·Å^{-3})	0.69/-0.47	0.34/-0.24

4. ^{1}H NMR Titration Experiments of Ligands 2 and 3

To understand the coordination behaviors of ligands **2** and **3** towards Ag(I), we carried out ^{1}H NMR titration Experiments. Since the metal salt $AgBF_4$ hardly dissolves into $CHCl_3$ to produce a mM concentration solution, ^{1}H NMR titration experiments were carried out in the mixture solvents of $CDCl_3$/acetone-d_6 (v/v = 9:1). Such experiments could not provide reliable association affinities but revealed the binding profiles of silver cation to the ligands. To a solution of the ligand (2 mM, 0.5 mL) in $CDCl_3$/acetone-d_6 (v/v = 9:1), a solution of $AgBF_4$ (100 mM) in same mixture solvents was gradually added. In this process, a series of ^{1}H NMR spectra of the sample was recorded by ^{1}H NMR spectrometer at 298 K.

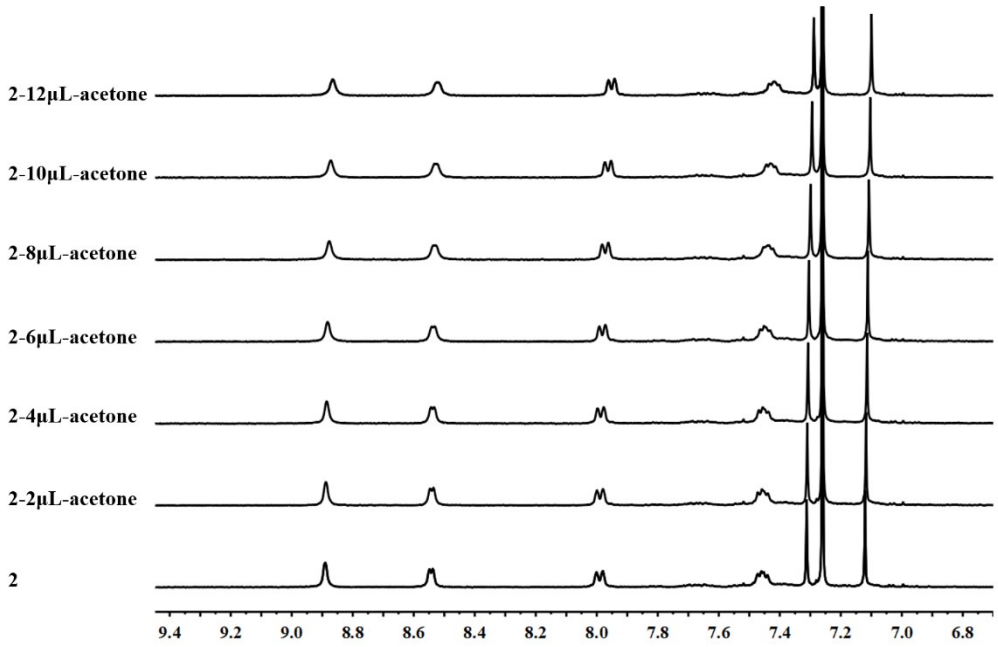

Figure S2. ^{1}H NMR titration spectra (400 MHz, 298 K) of **2** (2 mM) in $CDCl_3$ upon adding aliquots of acetone-d_6.

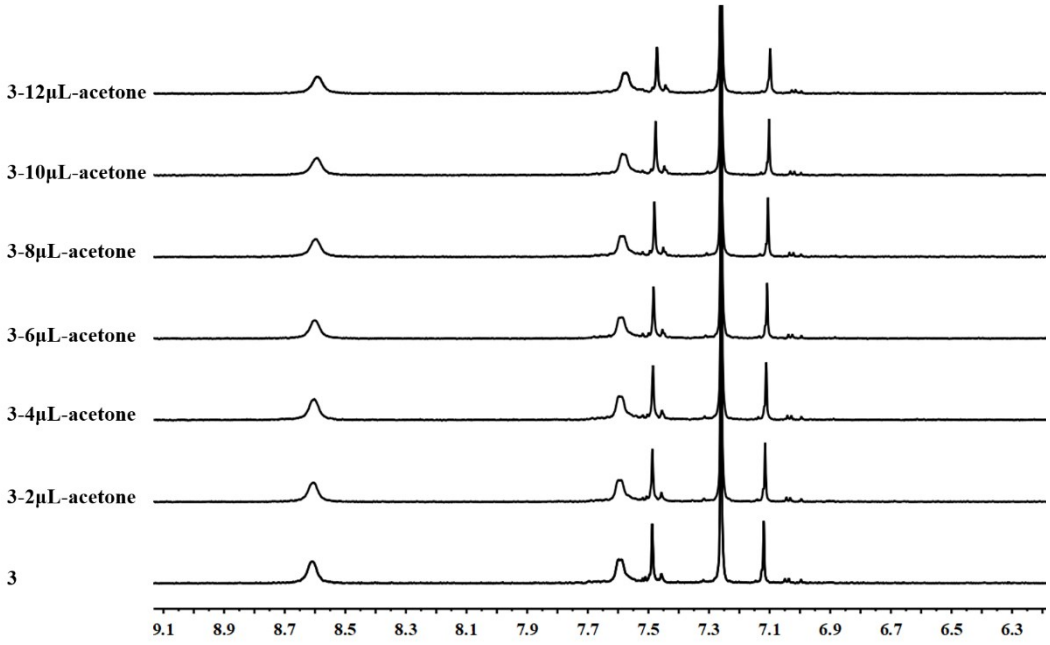

Figure S3. ^{1}H NMR titration spectra (400 MHz, 298 K) of **3** (2 mM) in $CDCl_3$ upon adding aliquots of acetone-d_6.

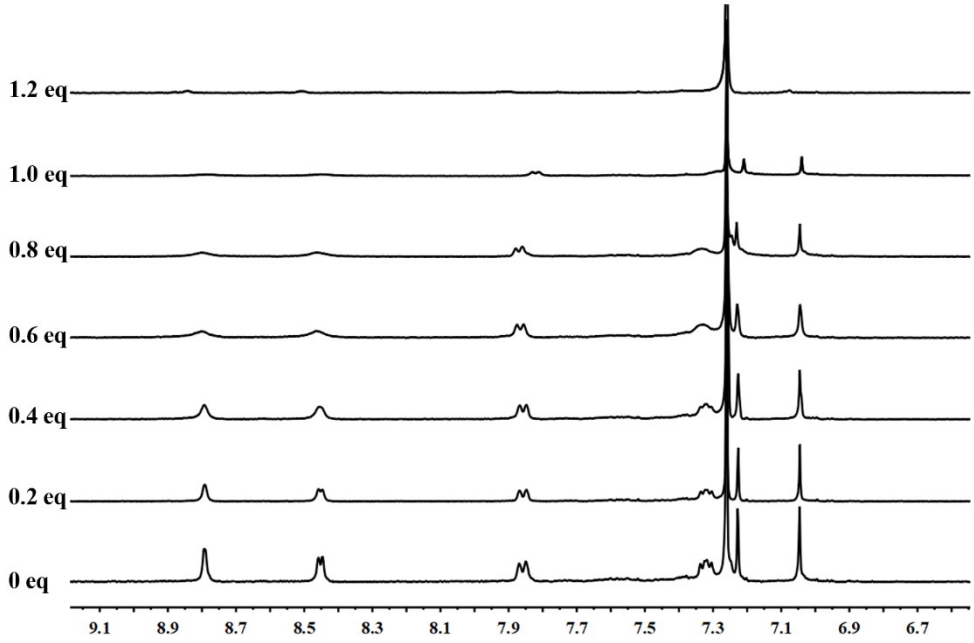

Figure S4. ^{1}H NMR titration spectra (400 MHz, 298 K) of **2** (2 mM) in $CDCl_3$/acetone-d_6 (v/v = 9:1) upon adding aliquots of $AgBF_4$ (100 mM) in same mixture solvents.

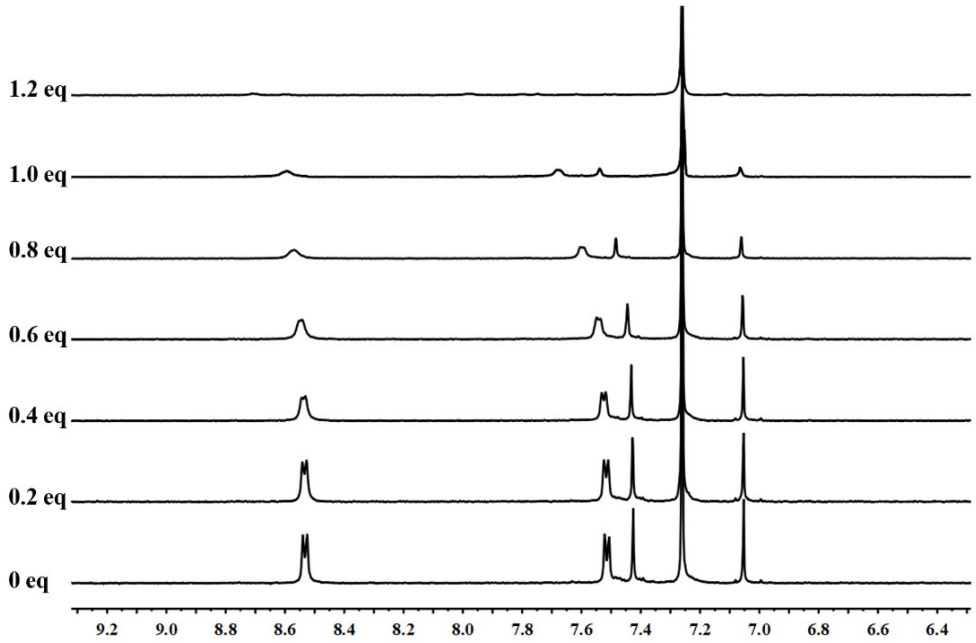

Figure S5. ^{1}H NMR titration spectra (400 MHz, 298 K) of **3** (2 mM) in $CDCl_3$/acetone-d_6 (v/v = 9:1) upon adding aliquots of $AgBF_4$ (100 mM) in same mixture solvents.

5. Photographs of Metallogels 2Ag and 3Ag

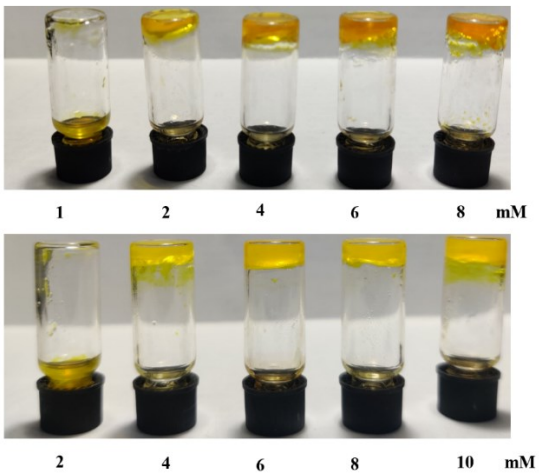

Figure S6. Photographs of gelation tests after ligands **2** and **3** are respectively coordinated with $AgBF_4$ at different concentrations (solvent: chloroform).

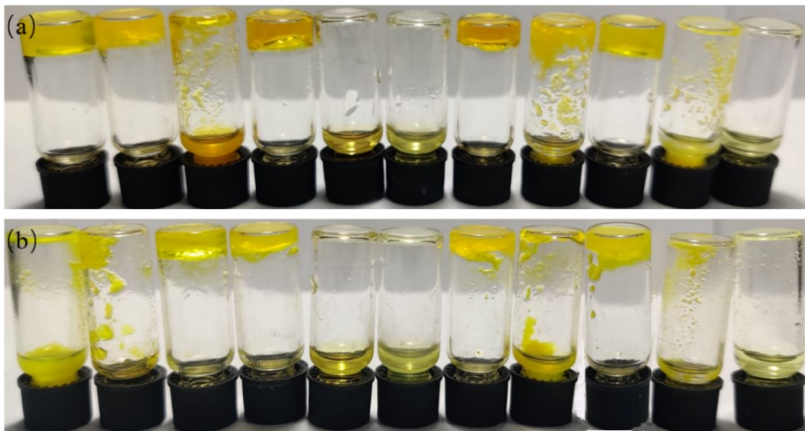

Figure S7. Photographs of gelation tests of Ligands **2** (a) and **3** (b) and $AgBF_4$ after coordination in different organic solvents (from left to right: ethanol, ethyl acetate, toluene, tetrahydrofuran, N, N-dimethylformamide, dimethyl sulfoxide, chloroform, 1,4-dioxane, acetone, n-hexane and acetonitrile).

Table S2. Gelation of two ligands with $AgBF_4$ in different solvents at room temperature.

solvent	**2** + Ag(Ⅰ)	**3** + Ag(Ⅰ)
ethanol	G[a]	PG
ethyl acetate	G	PG
toluene	PG[b]	G
tetrahydrofuran	G	G
N, N-dimethylformamide	S[c]	S
dimethyl sulfoxide	S	S
chloroform	G	G
1,4-dioxane	PG	PG
acetone	G	G
n-hexane	P[d]	P
acetonitrile	S	S

G[a]: gel, PG[b]: partial gel, S[c]: solution, P[d]: Precipitate.

6. Rheology measurements

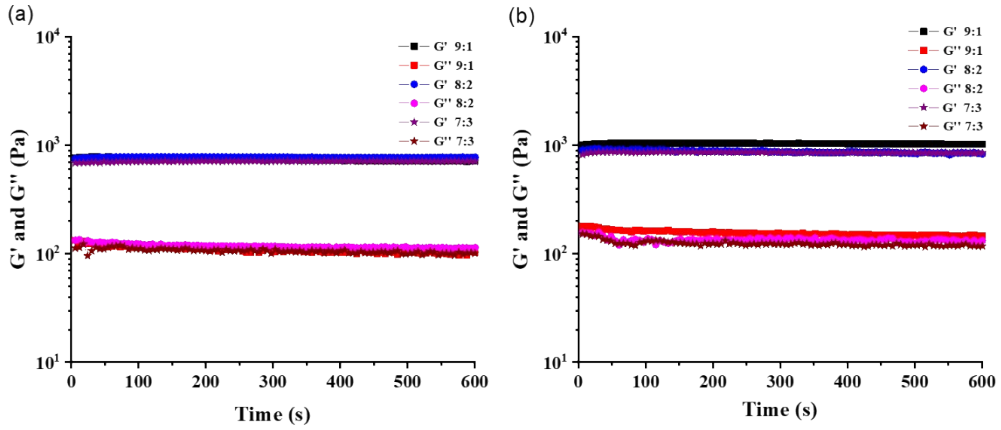

Figure S8. Rheology measurements of gels (a) **2Ag** and (b) **3Ag** obtained in different volume ratio of chloroform and acetone (frequency of 1Hz and strain of 0.1%, 4 mM at 10 ^{o}C).

7. FT-IR Spectra of Ligand 3 and Metallogel 3Ag

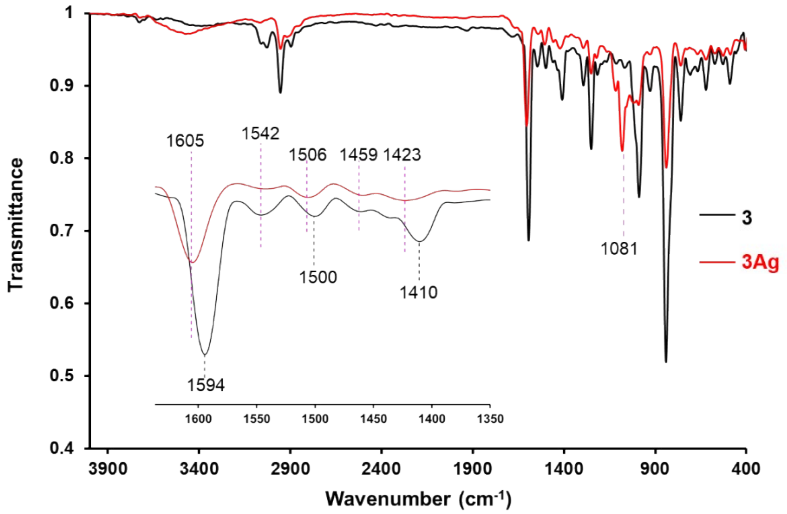

Figure S9. Comparison of FT-IR Spectra of ligand **3** and gel **3Ag**.

8. UV-vis/PL Titration Experiments

To further understand the coordination behaviors and optical behaviors of ligands **2** and

3 towards Ag(I), we carried out UV-vis/PL titration Experiments. Since the metal salt $AgBF_4$ hardly dissolves into $CHCl_3$ to produce a mM concentration solution, UV-vis/PL titration experiments were carried out by a gradual addition of the concentrated solution of silver in acetone to the ligand in $CHCl_3$. To a solution of the ligand (10 μM, 2 mL) in $CHCl_3$, a solution of $AgBF_4$ (2 mM) in acetone was gradually added. In this process, a series of UV-vis/PL spectra of the sample was recorded by UV-vis/PL spectrometer at 298 K.

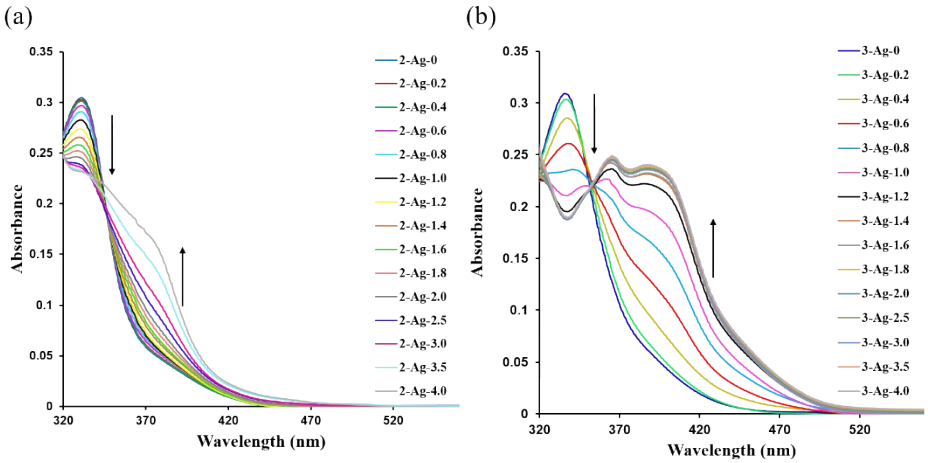

Figure S10. (a) Changes of partial UV-vis spectra of **2** (1E-5 M, in $CHCl_3$) upon adding of $AgBF_4$ in acetone (λ_{max} = 376 nm); (b) Changes of partial UV-vis spectra of **3** (1E-5 M, in $CHCl_3$) upon adding of $AgBF_4$ in acetone (λ_{max} = 390 nm).

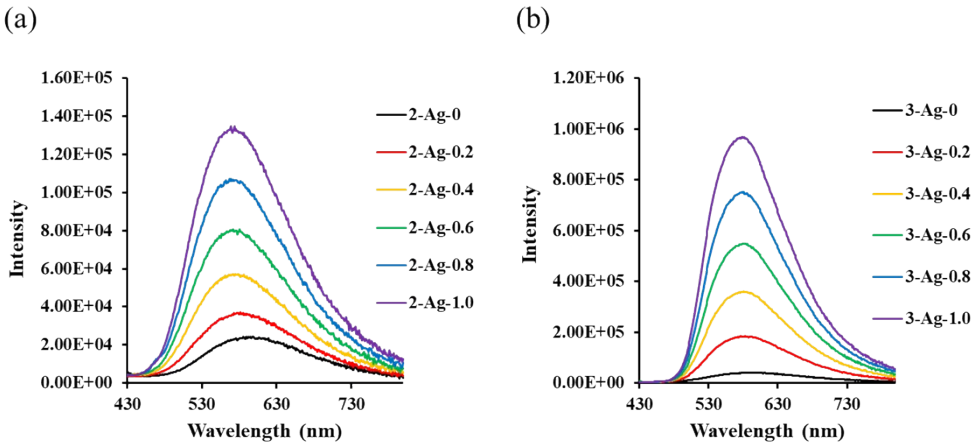

Figure S11. Changes of partial PL spectra of **2** (a) and **3** (b) (1E-5 M, in $CHCl_3$) upon adding of $AgBF_4$ (2 mM, in acetone).

9. XPS of 2Ag and 3Ag

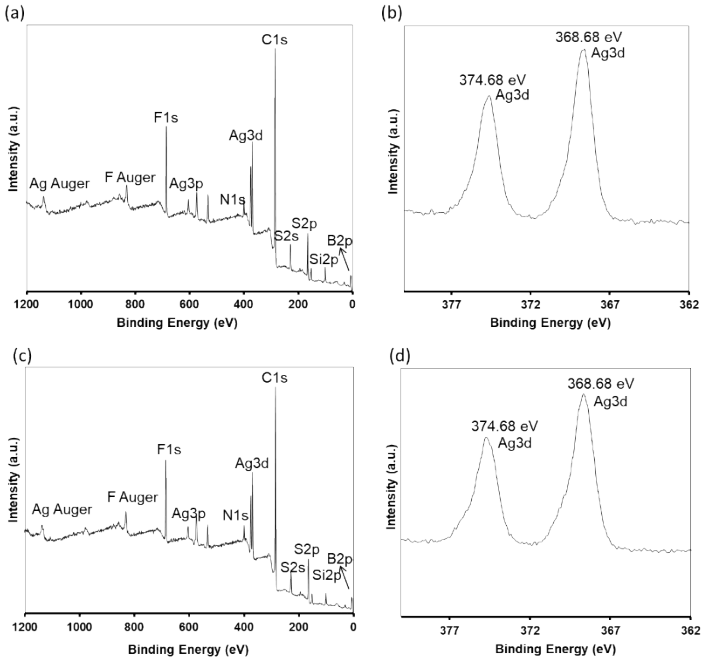

Figure S12. (a) XPS spectrum of **2Ag**; (b) XPS spectrum of Ag 3d in **2Ag**; (c) XPS spectrum of **3Ag**; (d) XPS spectrum of Ag 3d in **3Ag**.

10.TEM and SEM images of 2 and 3

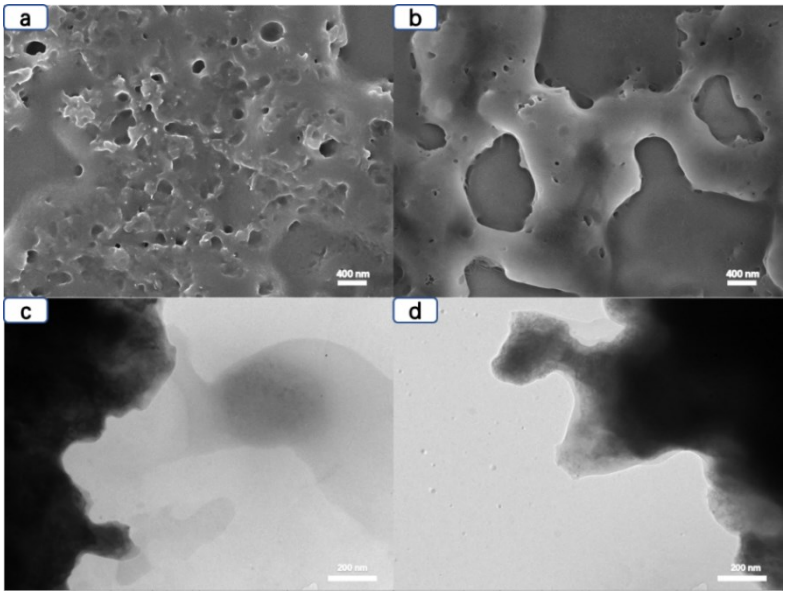

Figure S13. SEM images of compounds (a) **2** and (b) **3**; TEM images of compounds

(c) **2** and (d) **3**.

11. AFM images of 2Ag and 3Ag

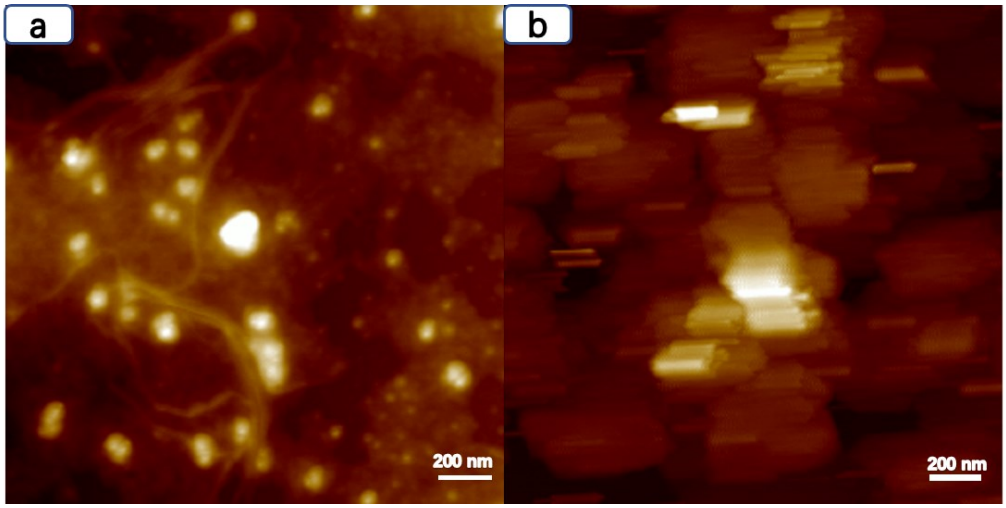

Figure S14. AFM images of (a) **2Ag** and (b) **3Ag**.

12. The Gel-sol Transitions of 2Ag and 3Ag Triggered by Different Stimuli

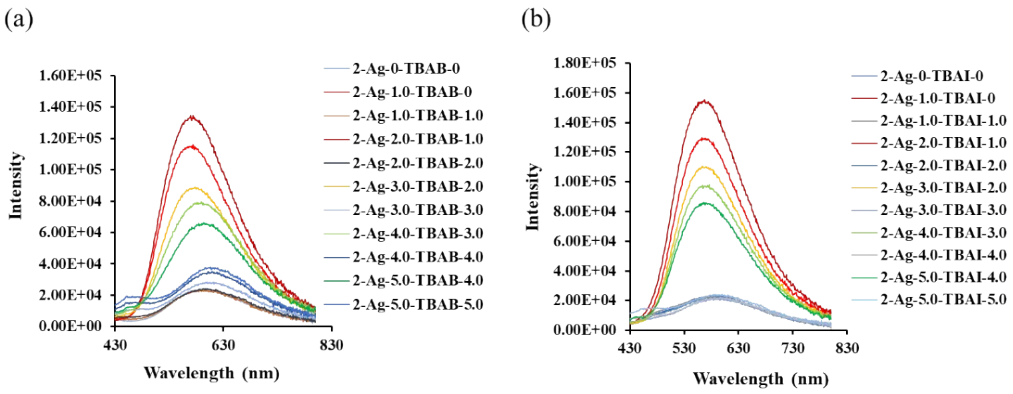

Figure S15. Fluorescence titration of mutual conversion between **2** and **2Ag** in dilute solution by addition of TBAB and TBAI (solvent: chloroform).

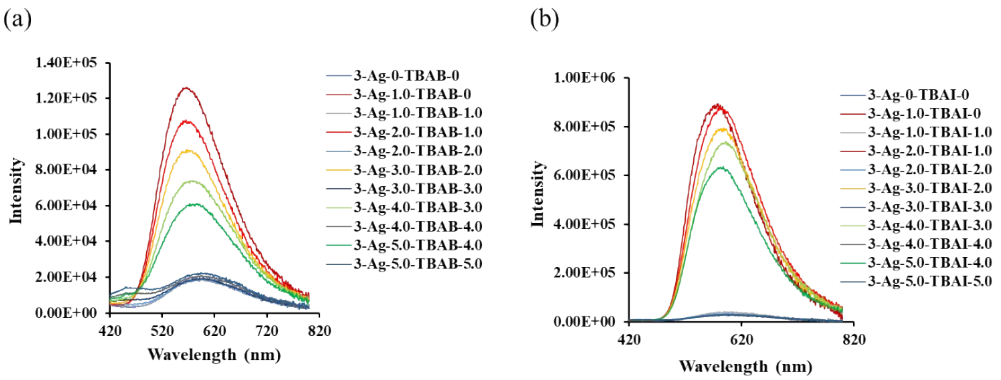

Fig. S16. Fluorescence titration of mutual conversion between **3** and **3Ag** in dilute solution by addition of TBAB and TBAI. (solvent: chloroform).

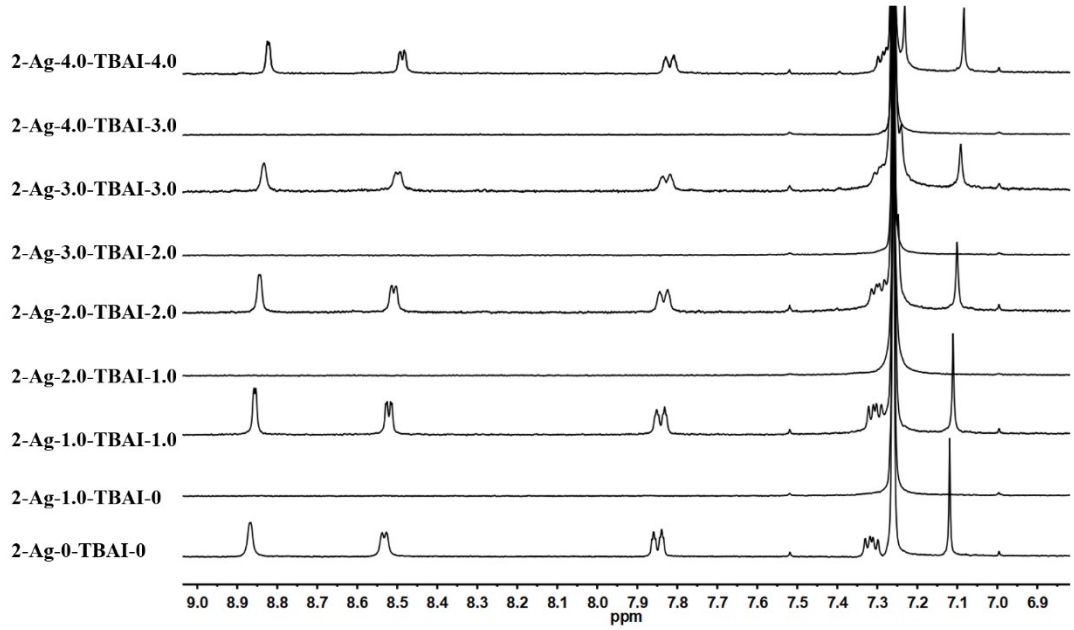

Figure S17. ^{1}H NMR titration spectra (400 MHz, $CDCl_3$, 298 K) of mutual conversion between **2** (2 mM) and **2Ag** by addition of TBAI.

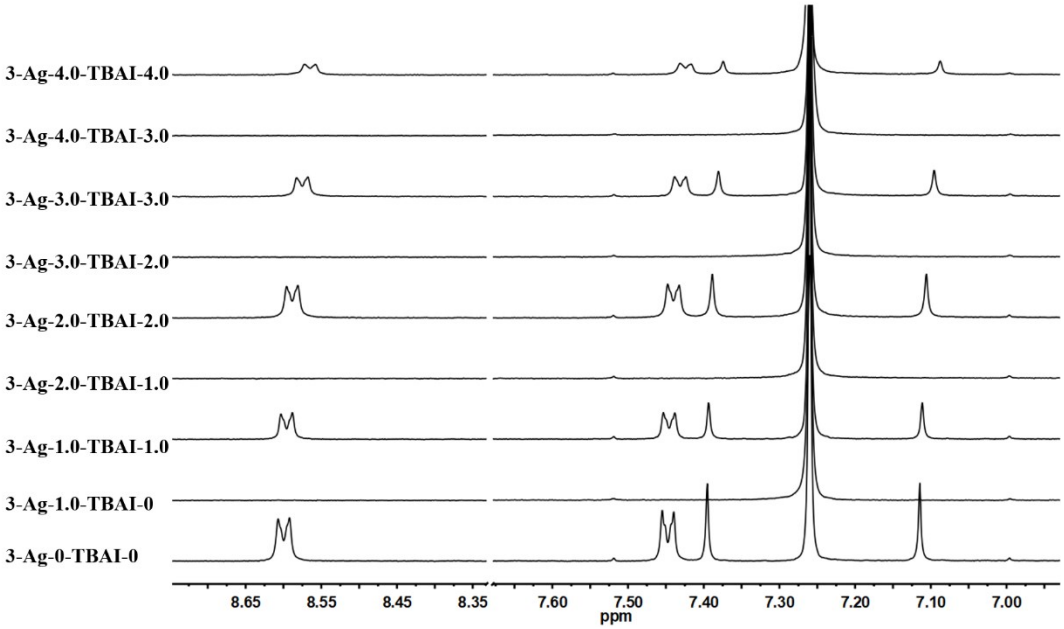

Figure S18. ^{1}H NMR titration spectra (400 MHz, $CDCl_3$, 298 K) of mutual conversion between **3** (2 mM) and **3Ag** by addition of TBAI.

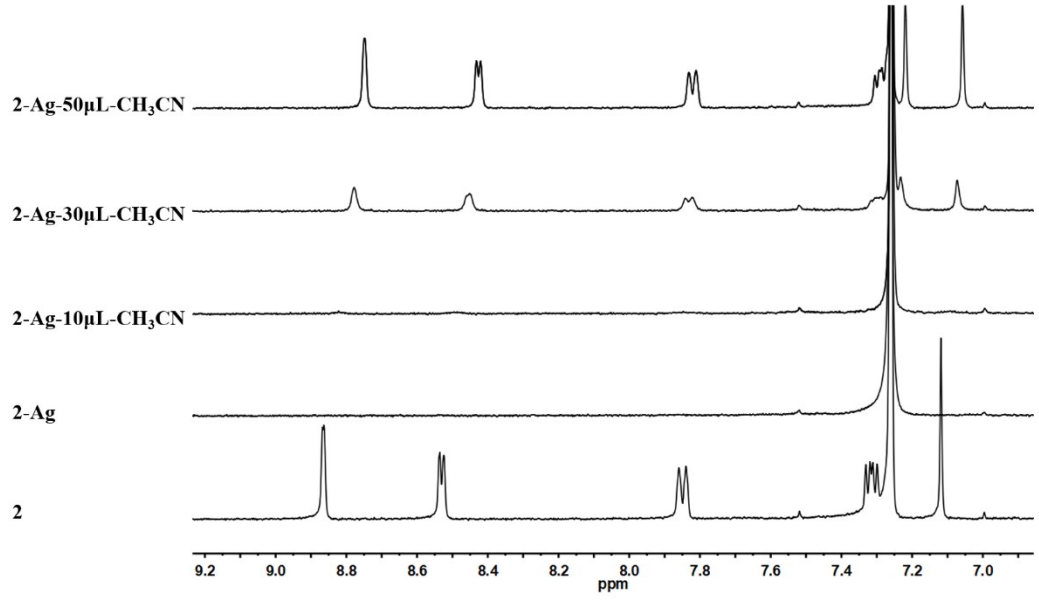

Figure S19. Changes of partial ^{1}H NMR spectra (400 MHz, $CDCl_3$, 298 K) of **2** (2 mM) upon adding of Ag^+ and acetonitrile-d_3.

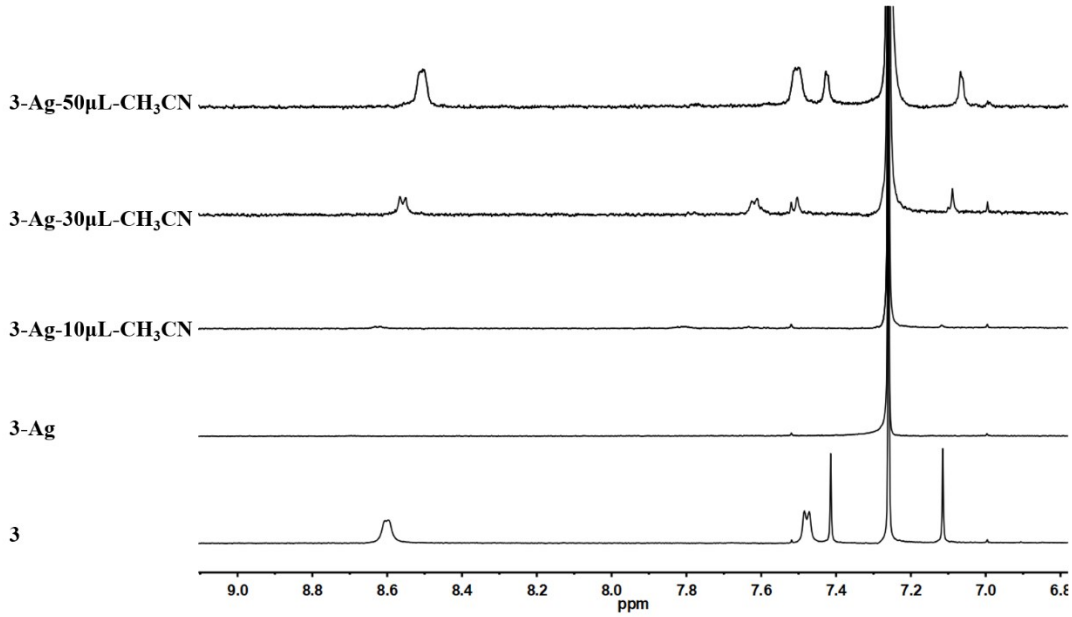

Figure S20. Changes of partial ^{1}H NMR spectra (400 MHz, $CDCl_3$, 298 K) of **3** (2 mM) upon adding of Ag^+ and acetonitrile-d_3.

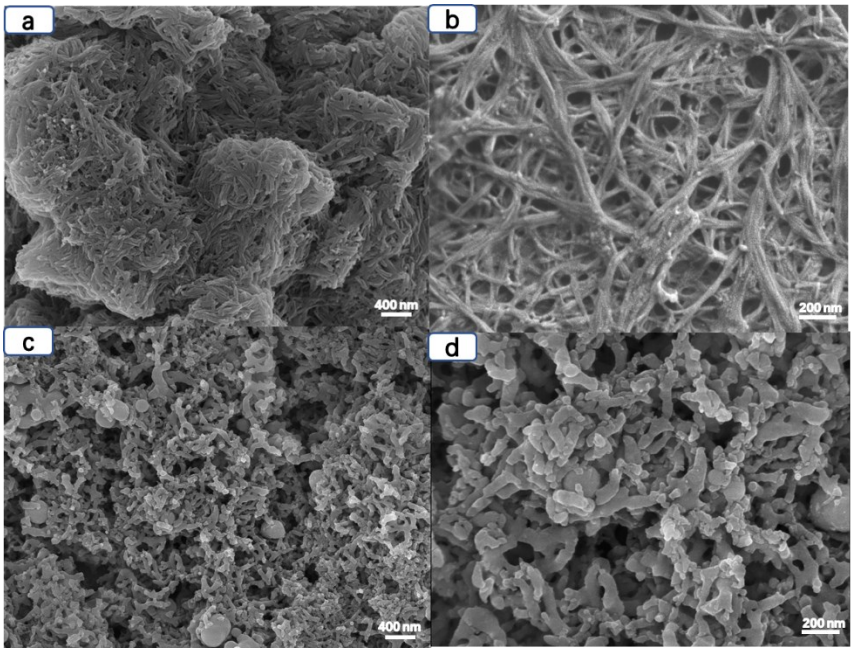

Figure S21. SEM images of metallogel **2Ag** at (a) 400 nm and (b) 200 nm magnifications; SEM images of metallogel **2Ag** by addition of 200 eq acetonitrile at (c) 400 nm and (d) 200 nm magnifications.

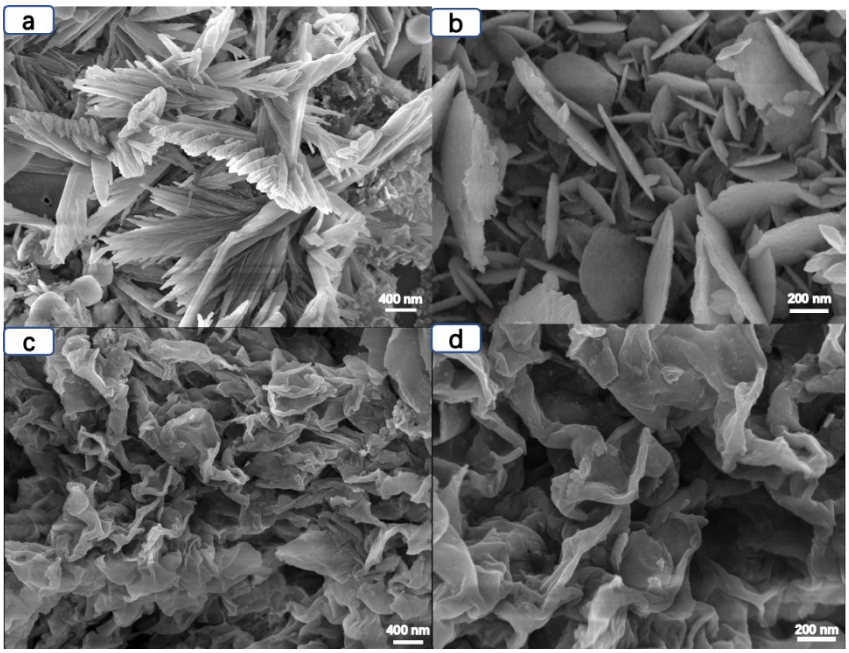

Figure S22. SEM images of metallogel **3Ag** at (a) 400 nm and (b) 200 nm magnifications; SEM images of metallogel **3Ag** by addition of 200 eq acetonitrile at (c) 400 nm and (d) 200 nm magnifications.

13. AIE Behaviors and the Gel-sol Transitions of 2Ag and 3Ag Triggered by H_2O

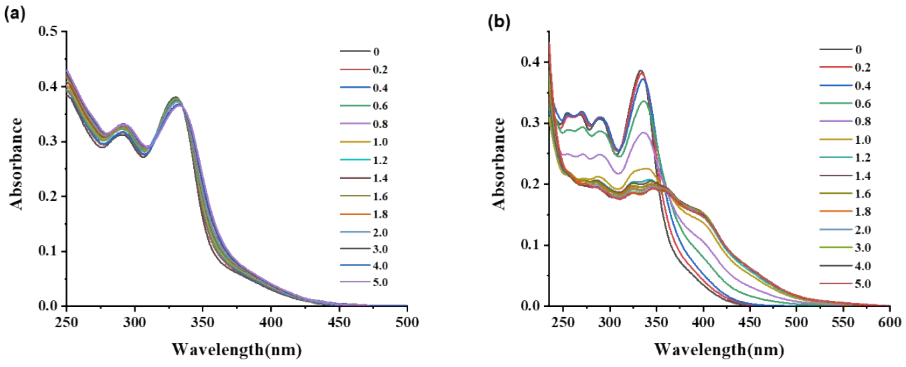

Figure S23. (a) Changes of partial UV-vis spectra of **2** (1E-5 M, in THF) upon adding of $AgBF_4$ (λ_{max} = 331 nm); (b) Changes of partial UV-vis spectra of **3** (1E-5 M, in THF) upon adding of $AgBF_4$ (λ_{max} = 338 nm). (solvent: tetrahydrofuran).

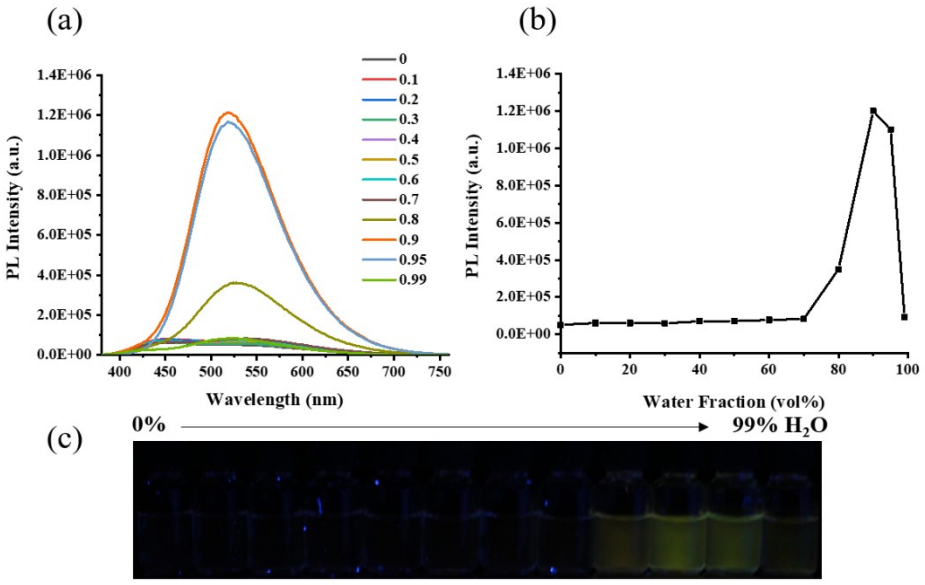

Figure S24. (a) The PL spectra of **2** ([C] = 1E-5 M) in THF/water mixtures with different water fractions; λex = 331 nm; (b) The changes of PL peak intensities at 520 nm vs the water fraction in the THF/water mixtures. (c) Fluorescence photos of the corresponding luminogens in THF/water mixtures (fw = 0 to 99 vol%), taken under the illumination of a UV lamp (365 nm).

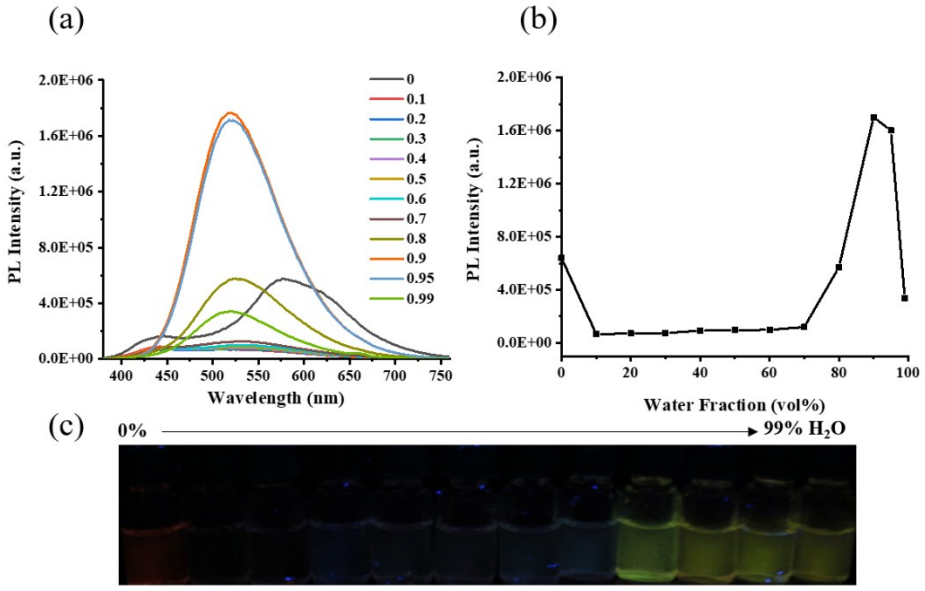

Figure S25. (a) The PL spectra of **2Ag** ([C] = 1E-5 M) in THF/water mixtures with different water fractions; λex = 331 nm; (b) The changes of PL peak intensities at 520 nm vs the water fraction in the THF/water mixtures. (c) Fluorescence photos of the corresponding luminogens in THF/water mixtures (fw = 0 to 99 vol%), taken under the illumination of a UV lamp (365 nm).

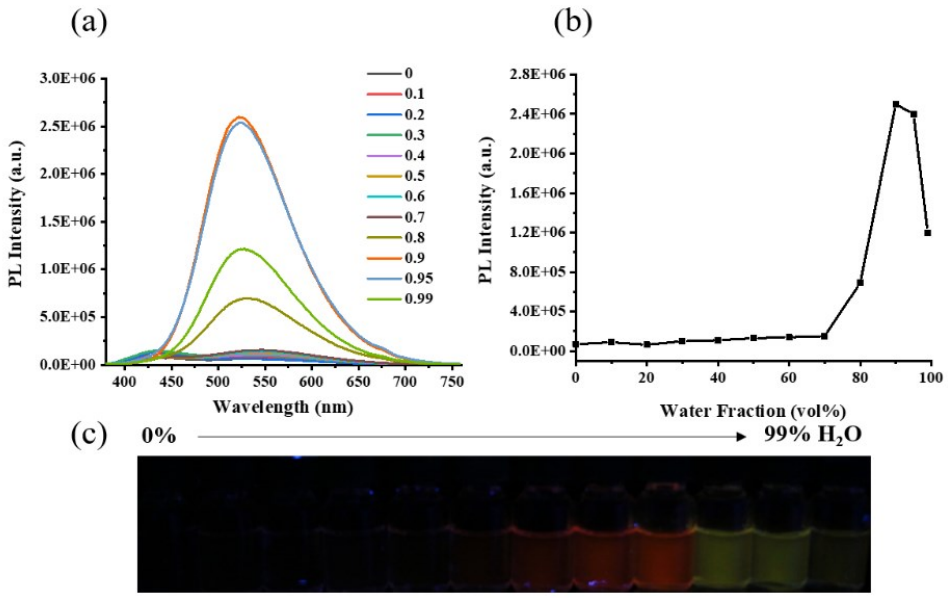

Figure S26. (a) The PL spectra of **3** ([C] = 1E-5 M) in THF/water mixtures with different water fractions; λex = 338 nm; (b) The changes of PL peak intensities at 520 nm vs the water fraction in the THF/water mixtures. (c) Fluorescence photos of the corresponding luminogens in THF/water mixtures (fw = 0 to 99 vol%), taken under the illumination of a UV lamp (365 nm).

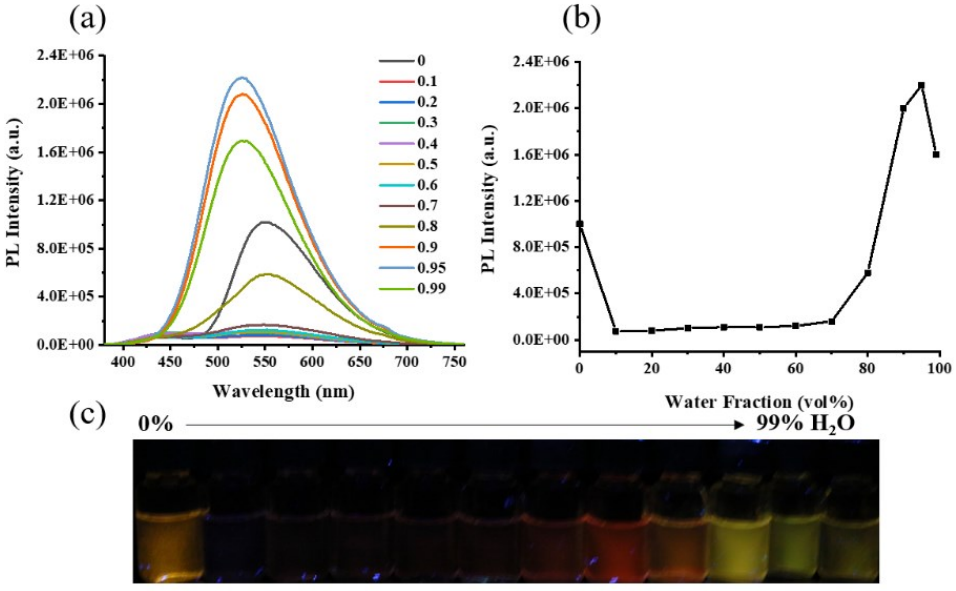

Figure S27. (a) The PL spectra of **3Ag** ([C] = 1E-5 M) in THF/water mixtures with different water fractions; λex = 338 nm; (b) The changes of PL peak intensities at 520 nm vs the water fraction in the THF/water mixtures. (c) Fluorescence photos of the corresponding luminogens in THF/water mixtures (fw = 0 to 99 vol%), taken under the illumination of a UV lamp (365 nm).

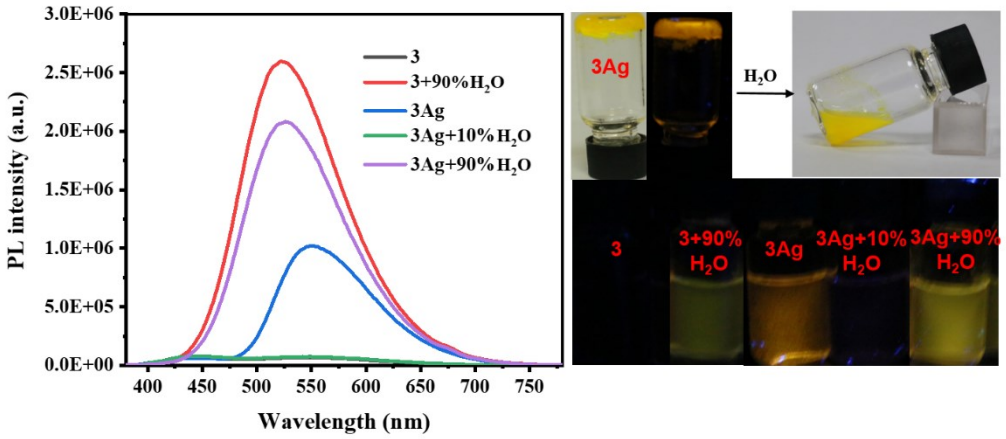

Figure S28. The gel–sol transitions of the supramolecular metallogels **3Ag** triggered by H_2O (Left: The PL spectra of **3** and **3Ag** ([C] = 1E-5 M) in THF and water; Right: Fluorescence and gel–sol transition photos; **3**: λ_{em} = 440 nm; **3Ag**: λ_{em} = 540 nm; **3+90%H_2O**: λ_{em} = 524 nm).

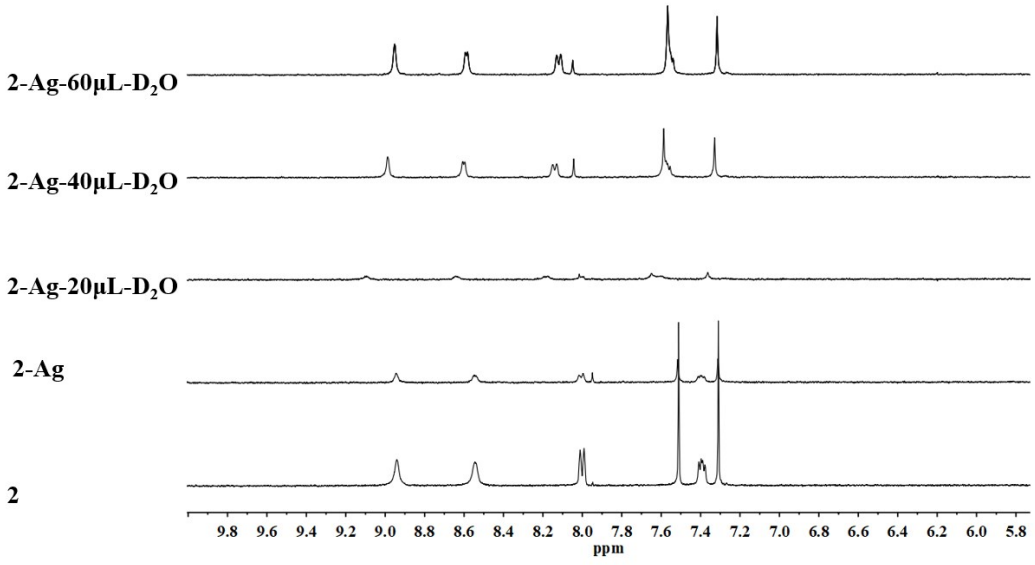

Figure S29. Changes of partial ^{1}H NMR spectra (400 MHz, THF-d_8, 298 K) of **2** (2 mM) upon adding of Ag^+ and D_2O.

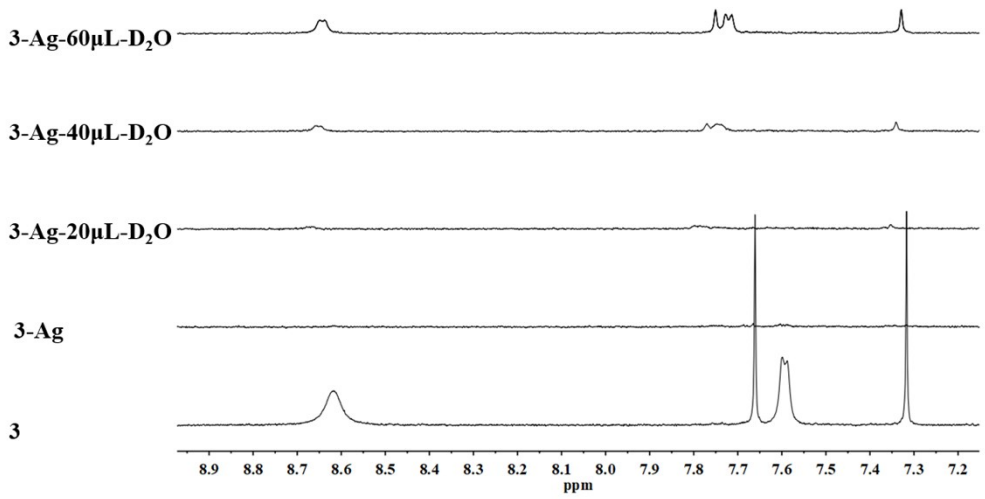

Figure S30. Changes of partial ^{1}H NMR spectra (400 MHz, THF-d_8, 298 K) of **3** (2 mM) upon adding of Ag^+ and D_2O.

14. NMR / HRMS and IR Spectra

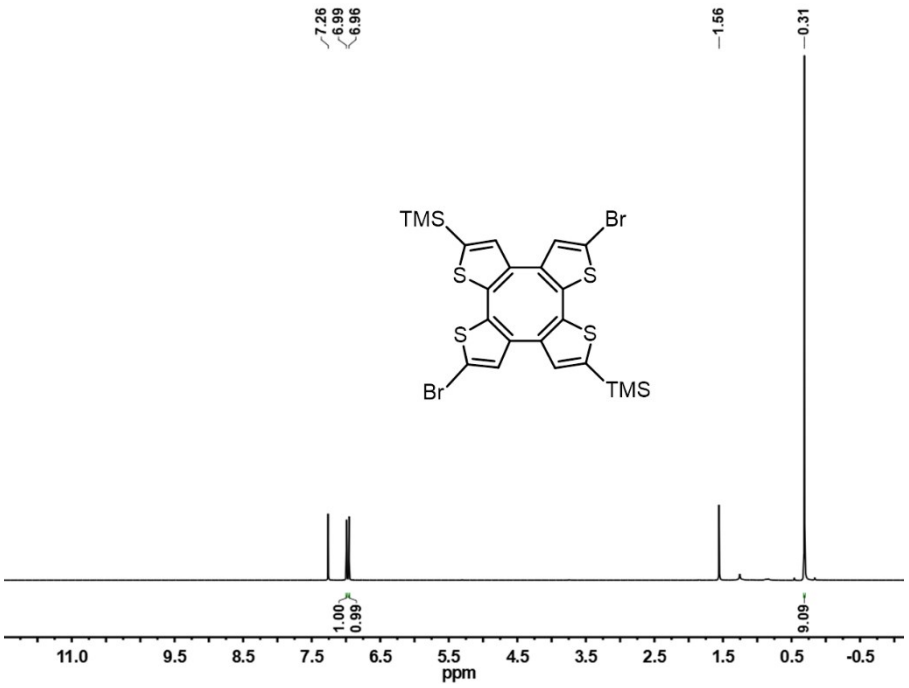

Figure S31. ^{1}H NMR (400 MHz, $CDCl_3$) spectrum of **6**.

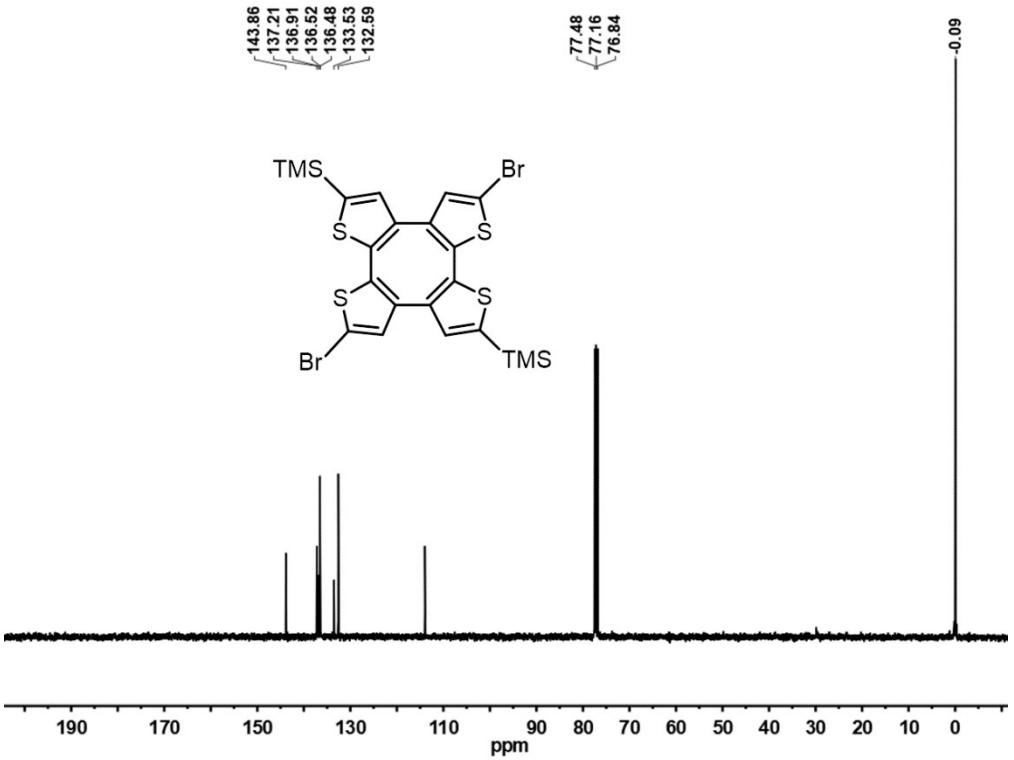

Figure S32. ^{13}C NMR (100 MHz, $CDCl_3$) spectrum of **6**.

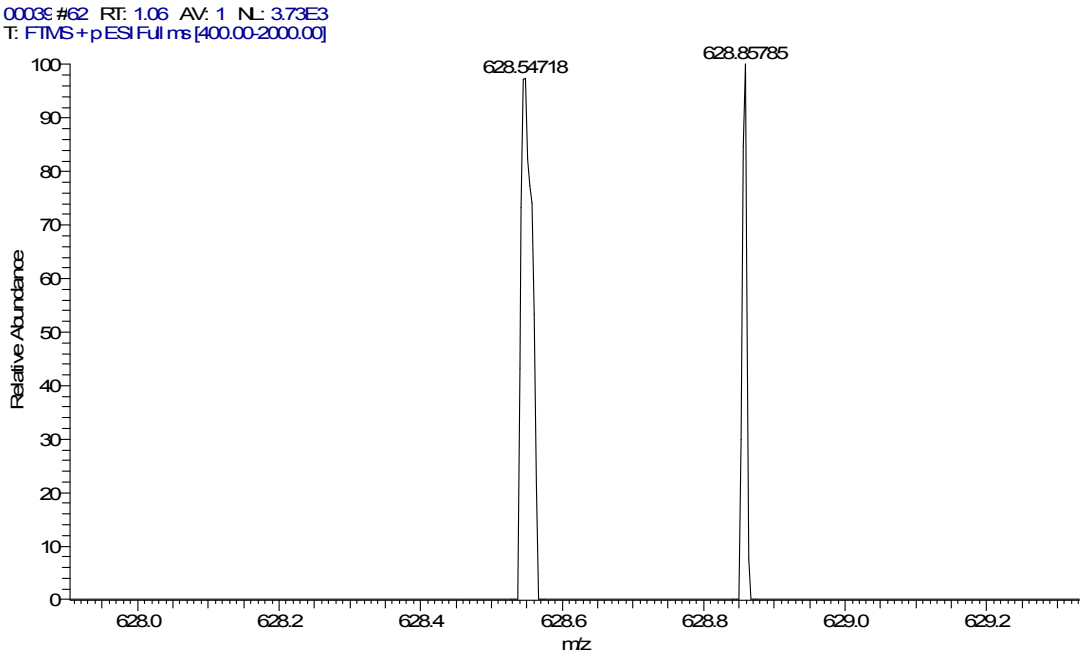

Figure S33. HRMS-ESI spectrum of **6**.

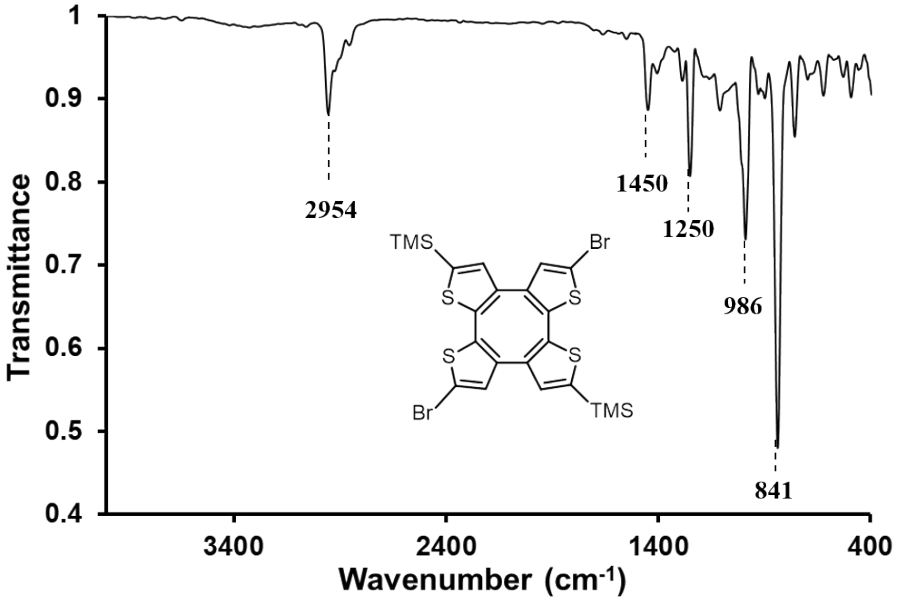

Figure S34. IR spectrum of compound **6**.

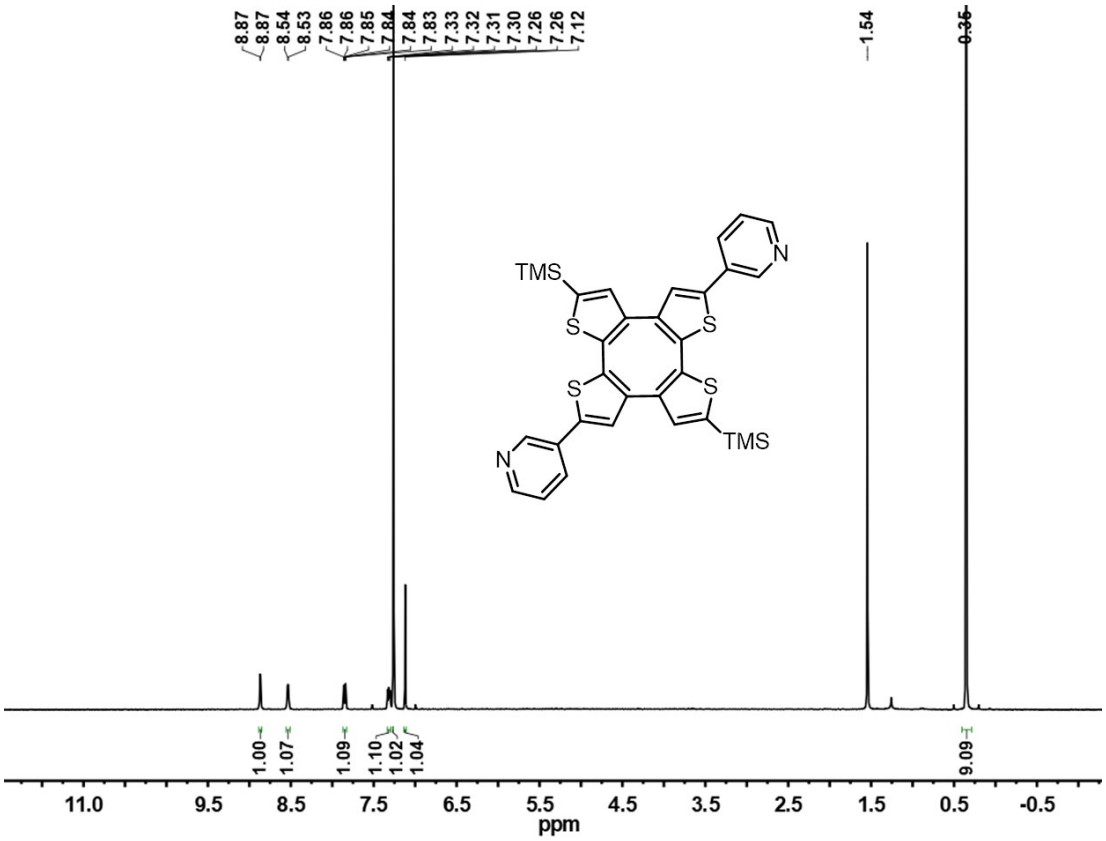

Figure S35. ^{1}H NMR (400 MHz, $CDCl_3$) spectrum of **2**.

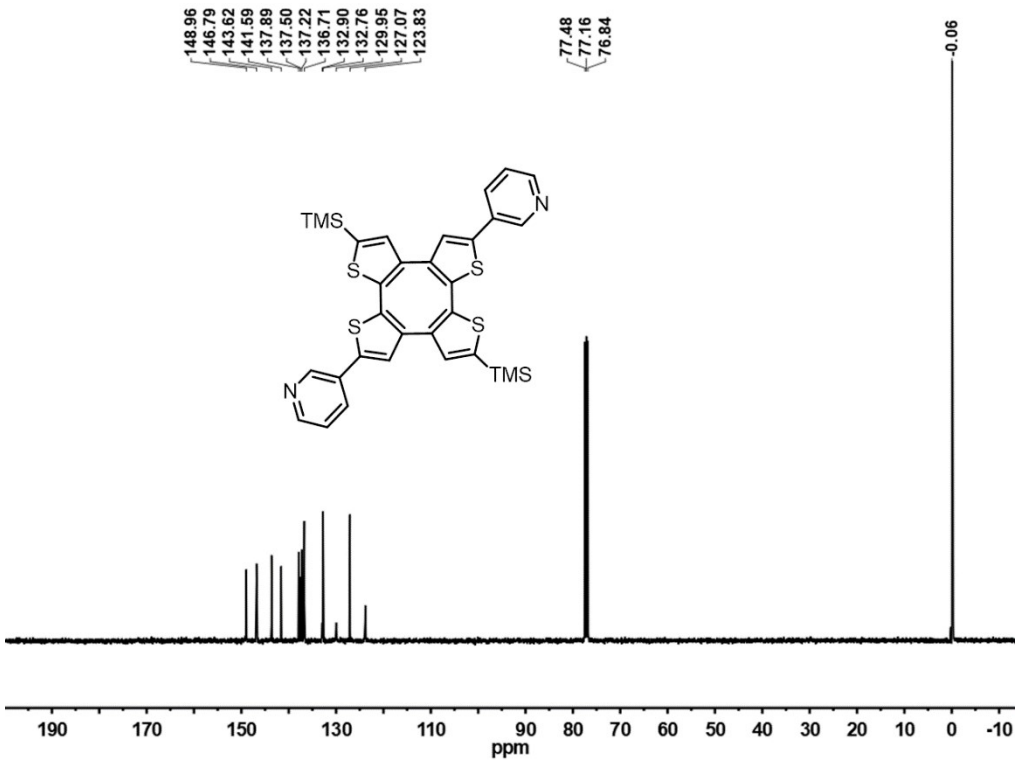

Figure S36. ^{13}C NMR (100 MHz, $CDCl_3$) spectrum of **2**.

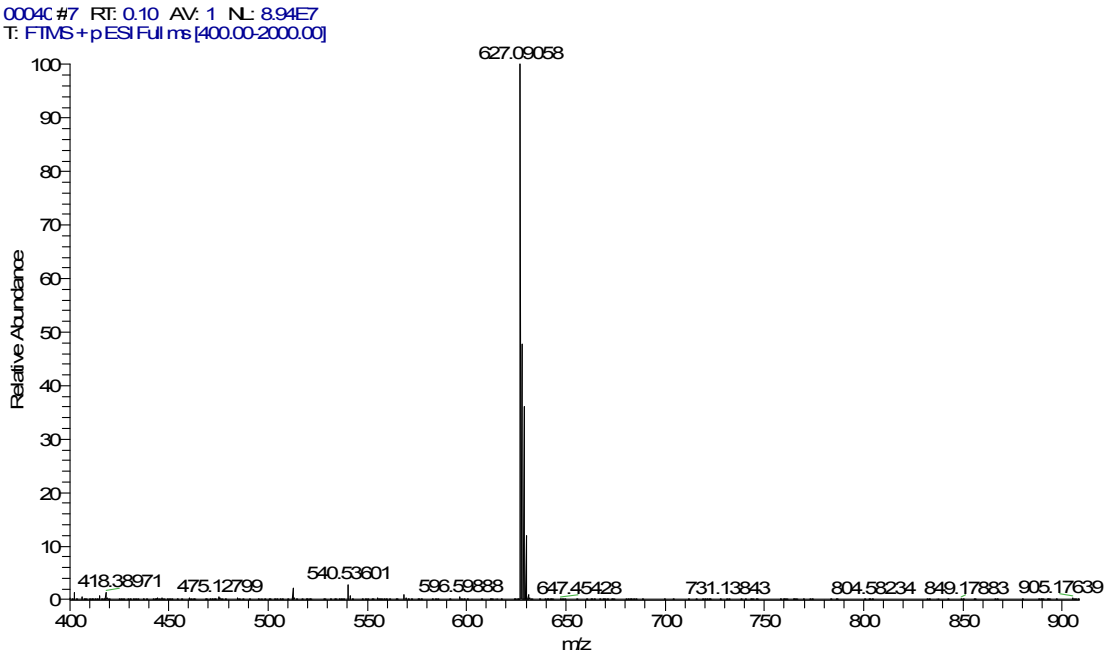

Figure S37. HRMS-ESI spectrum of **2**.

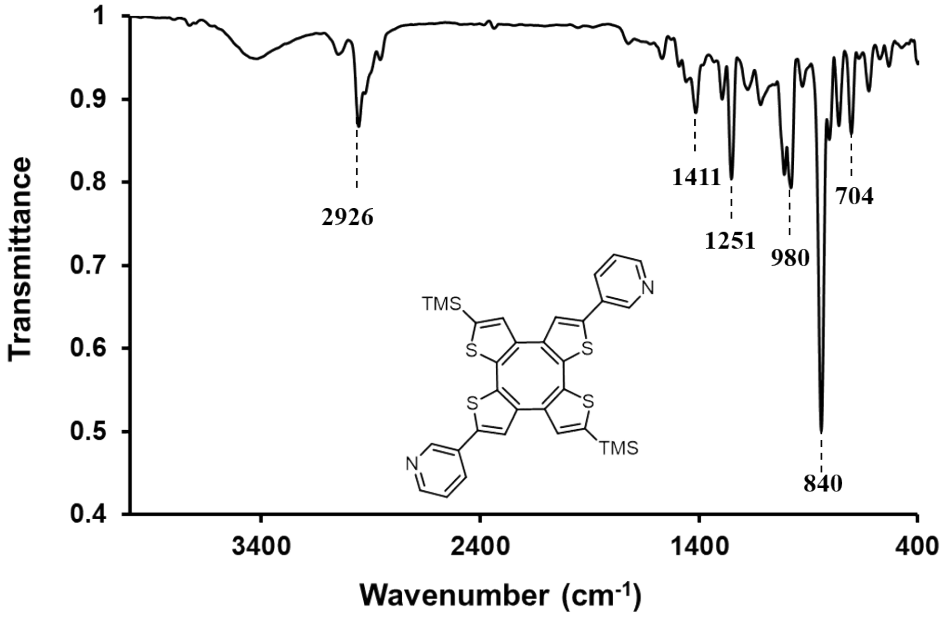

Figure S38. IR spectrum of compound **2**.

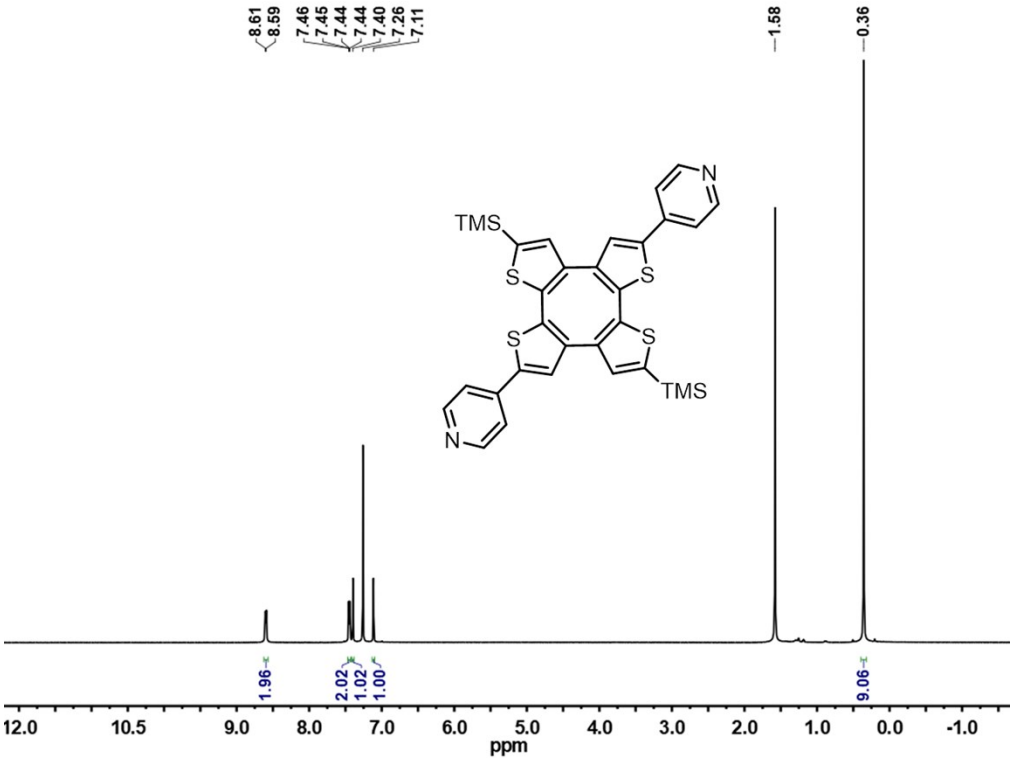

Figure S39. ^{1}H NMR (400 MHz, $CDCl_3$) spectrum of **3**.

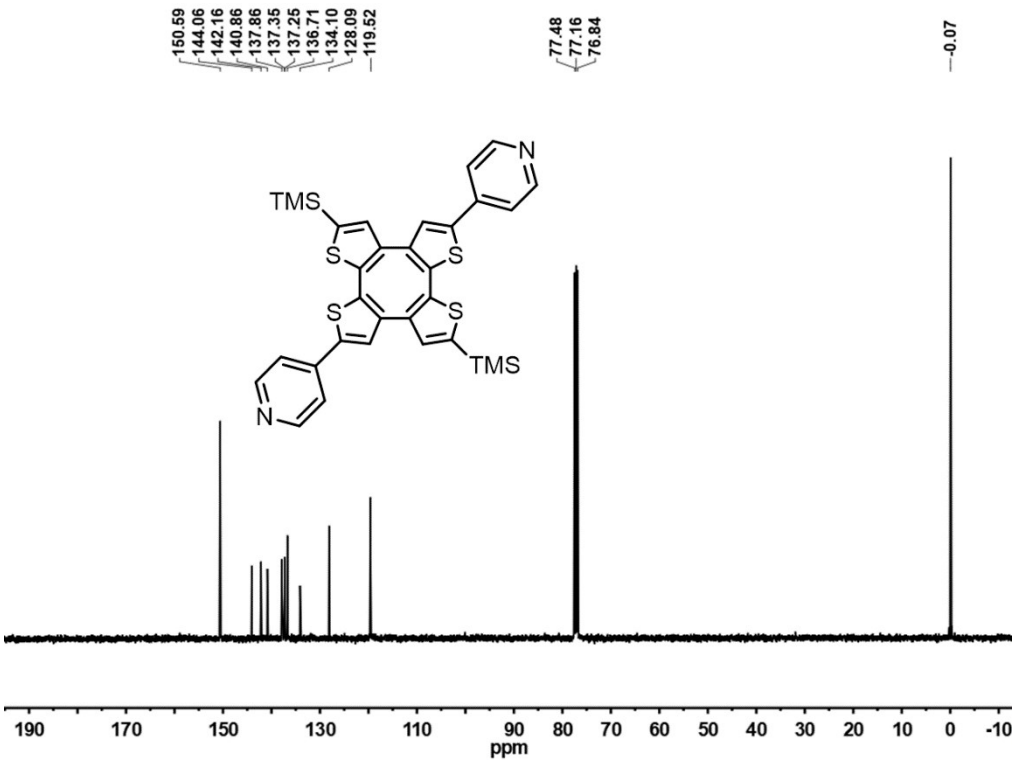

Figure S40. ^{13}C NMR (100 MHz, $CDCl_3$) spectrum of **3**.

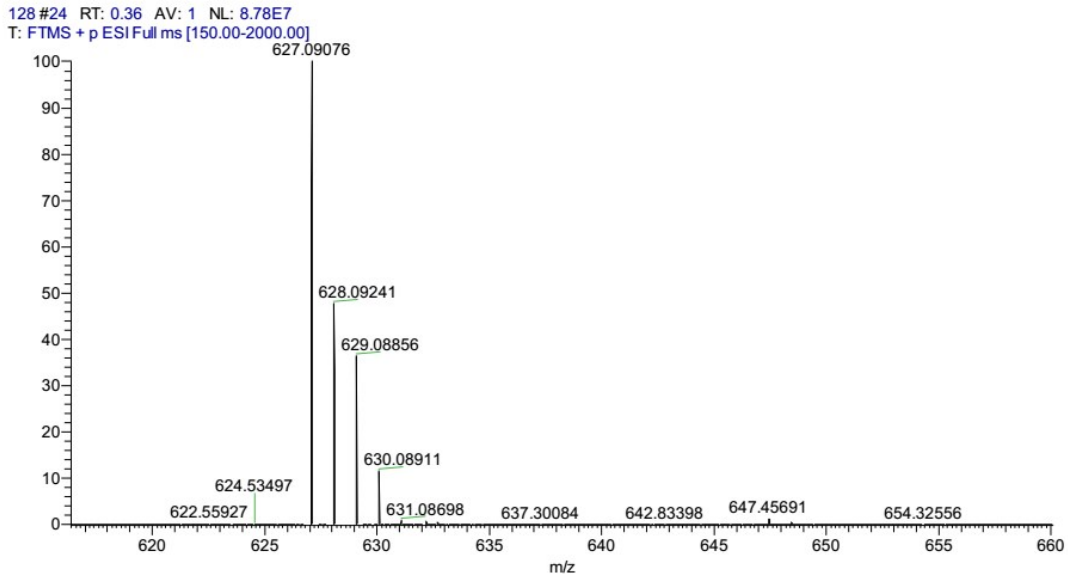

Figure S41. HRMS-ESI spectrum of **3**.

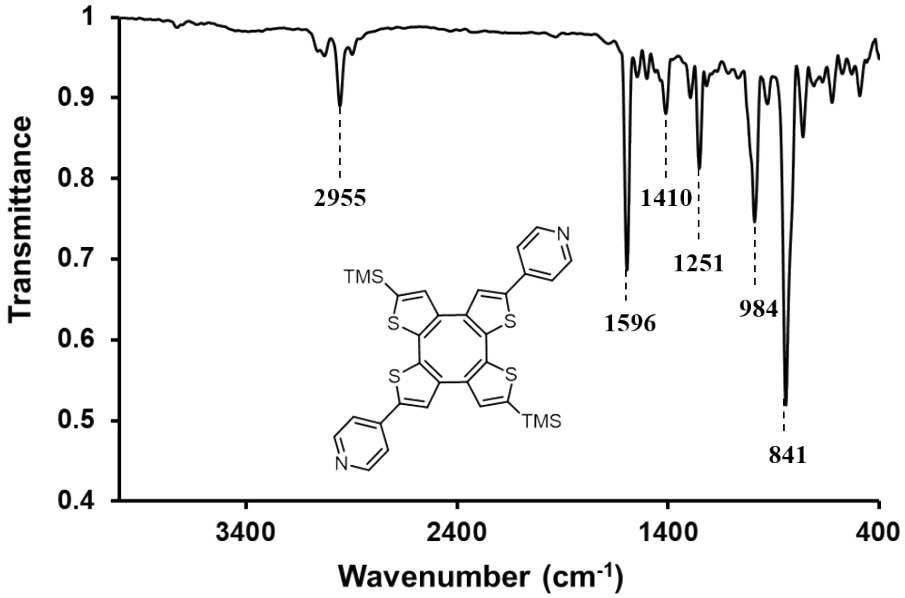

Figure S42. IR spectrum of compound **3**.

15. Reference

[1] Suffert, J. *J. Org. Chem.* **1989**, *54*, 509.

[2] Greviiig, B.; Woltermann, A.; and Kautfmann, T. *Angew. Chem. Int. Ed.*, **1974**, *13*, 467.

[3] Tian, Y.; Wang, G. X.; Ma, Z. Y.; Xu, L.; Wang, H. *Chem. Eur. J.* **2018**, *24*, 15993.